Compression- and Shear-Induced Polymerization in Model Diacetylene-Containing Monolayers

Ginger M. Chateauneuf,[†] Paul T. Mikulski,[‡] Guang-Tu Gao,[†] and Judith A. Harrison*,[†]

Departments of Chemistry and Physics, United States Naval Academy, Annapolis, Maryland 21402

Received: May 4, 2004; In Final Form: August 5, 2004

Molecular dynamics simulations have been used to examine the response of monolayers composed of alkyne chains, which contain diacetylene moieties, to compression and shear. The simulations show that both compression and shear result in cross-linking, or polymerization, between chains. Irregular polymerization patterns appear among the carbon backbones. The vertical positioning of the diacetylene moieties within the alkyne chains (spacer length) and the sliding direction have an influence on the pattern of cross-linking and friction. In addition, chemical reactions between the chains of the monolayer and the amorphous carbon tip occur when diacetylene moieties are located at the ends of the chains closest to the tip. These adhesive interactions increase friction.

Introduction

The properties of single- and multilayer Langmuir–Blodgett (LB) films[1–5] and self-assembled monolayers (SAMs)[6–15] containing chains with diacetylene moieties have been the subject of much interest. This is largely due to the fact that exposure to UV radiation causes these films to become cross-linked, forming highly ordered structures of polydiacetylene (PDA) with long conjugated π-bonded backbones.[16] These structures have the potential to be used as molecular sensors because the cross-linked backbone demonstrates a chromatic response to elevated temperature and stress.[13,16–18] It has also been suggested that the polymerized region may increase the durability of the film[19] and that these monolayers have the potential to be used as photoresists for interfacial patterning.[12]

The spatial requirements of the diacetylene-containing chains needed to effectively polymerize in monolayers[8–11] are the same as they are in crystals.[16,18] In particular, the length of the spacer (between the substrate and the diacetylene moieties) must be able to accommodate the changes in hybridization that accompany crystallization. In LB films, because the monolayer is not chemically bound to the surface, the chains have a certain degree of mobility. As a result, the vertical positioning of the diacetylene moieties (spacer length) has little effect on polymerization; however, it does affect the length of the resultant backbone.[8] In contrast, Menzel et al.[11] examined the effect of spacer length on the polymerization of SAMs containing diacetylene moieties. Their results show that monolayers with odd-spacer lengths (5 and 9) preferentially form the blue-phase polymer (longer π-conjugation length); however, even-spacer lengths (4 and 6) predominantly led to the formation of the red-phase polymer (shorter π-conjugation length). The authors also noted that this odd–even effect may disappear for very long spacer lengths.

The atomic-scale friction of unpolymerized diacetylene and polymerized monolayers has also been examined.[19,20] The friction of the unpolymerized monolayers generally increased with load and depended on the length of the spacer and tail groups. Increasing the length of the tail group caused the monolayers to become more crystalline and reduced the friction. Decreasing the length of the spacer caused the friction to increase, especially at high loads. The friction versus load data also possessed a "steplike" structure. Polymerization caused this steplike structure to disappear. In addition, the friction force showed a wide variation with measurement location on the film. This difference was assigned to differences in polymer backbone alignment relative to the scanning direction. Carpick et al.[20] independently measured the friction of polydiacetylene monolayers using atomic force microscopy and determined it is about 300% larger when scanning perpendicular to the polymer backbone direction compared to scanning parallel to the backbone. Burns et al. have observed a blue-to-red transition in polydiacetylene monolayers on silicon oxide with the application of shear.[13]

In this work, we have used molecular dynamics (MD) simulations to examine the compression and friction of model SAMs composed of chains containing a diacetylene moiety. Because we use a potential energy function that is capable of modeling chemical reactions, cross-linking (polymerization) of the chains is possible.[21] The spacer length of the diacetylene moieties was varied, and the effects on polymerization and friction were examined. To our knowledge, these are the first reported cases of simulated load- and shear-induced polymerization.

Simulation Details

Model SAMs were constructed by covalently bonding 56 alkyne chains to diamond (111) substrates in the (2 × 2) packing arrangement. This system is tightly packed with an area of 21.9 Å^2 per chain[22] and has approximately the same packing density as alkanethiols on gold (111).[23] Each alkyne chain ($-C_n-C\equiv C-C\equiv C-C_m$) contains one diacetylene moiety (triple–single–triple bond sequence). The remaining carbon atoms in each chain are sp^3-hybridized. Three monolayers that differ in the location of the diacetylene moiety within the chains were examined. The triple-bond region is located near the center of each chain in two monolayers. These two monolayers have spacer lengths

* Corresponding author. E-mail: jah@usna.edu.
† Department of Chemistry.
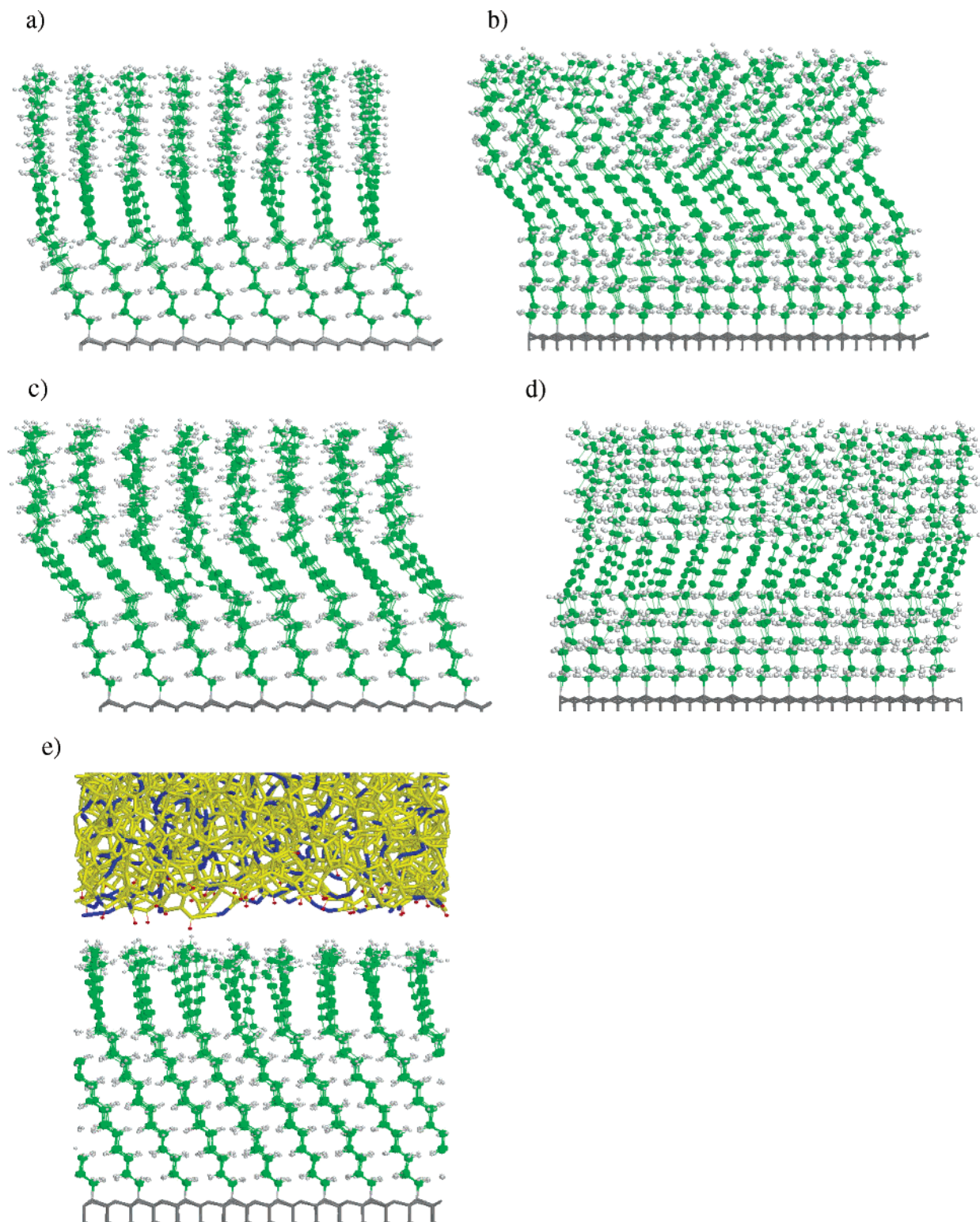‡ Department of Physics.

Figure 1. Perpendicular-chain (a and b) and tilted-chain (c and d) monolayers (tip omitted for clarity) at 300 K. The end-chain (e) monolayer plus the tip at 300 K. Gray wireframes represent the diamond (111) substrate. Green and gray spheres represent carbon and hydrogen atoms of the monolayers, respectively. Carbon atoms in the tip with sp-hybridization are blue, and all other carbon atoms in the tip are yellow. Hydrogen atoms in the tip are red spheres. Sliding from right-to-left in (b), (c), and (e) corresponds to the $-x$, y, and y directions, respectively. Sliding from right-to-left in (a) and from left-to-right in (d) corresponds to the y and x directions, respectively.

$(-C_n-)$ that differ by one carbon atom. In the perpendicular-chain and the tilted-chain monolayers (Figure 1a,b and 1c,d), 8 and 7 carbon atoms are between the diacetylene moiety and the diamond substrate, respectively. In the end-chain monolayer (Figure 1e), the diacetylene moieties are located on the ends of the chains closest to the probe with 14 carbon atoms separating the diacetylene moiety from the substrate.

The seven-layer diamond substrate contained 224 atoms per layer, with periodic boundary conditions applied in the plane that contains the monolayers. The dimensions of the computational cell were 35.21 Å by 34.85 Å in the x and y directions, respectively. Application of the thermostat has been done in the same way as described in our previous work.[22,24−28] Briefly, the diamond substrate was divided into regions such that the

bottom two layers were held rigid, a Berendsen thermostat[29,30] was applied to the next two layers (300 K), and the remaining top layers were free of constraints. It should also be noted that the results reported here are invariant to the type of thermostat used (i.e., Langevin thermostat yields the same results). Newton's equations of motion for all nonrigid atoms were integrated using a velocity Verlet algorithm.[31] The load and friction were taken to be the forces on the rigid-layer atoms that were normal to the plane containing the monolayer and parallel to the sliding direction, respectively.

Because the hydrogen-terminated amorphous-carbon probe does not have distinct layers, it was divided into three regions. The atoms in the outer, middle, and bottom regions were held rigid, had a thermostat applied (300 K), and had no constraints, respectively. The probe contains 1828 atoms (Figure 1e) and is composed of 64.3% sp^2-hybridized carbon, 12.5% sp^3-hybridized carbon, 20.1% sp-hybridized carbon, and 3.1% hydrogen atoms. Hydrogen atoms were used to terminate carbon atoms at the interface of the tip and the monolayer. The amorphous-carbon probe was created by randomly placing carbon atoms in the computational cell. The system was then heated and quenched while periodic boundary conditions were applied. This method is similar to the way in which amorphous films have previously been created.[32−34] At the surface of the tip (nearest the chains) unsaturated carbon atoms were removed or terminated with hydrogen atoms. This process yielded a randomized tip with enough variation in surface structure so the probe and the chains were incommensurate.
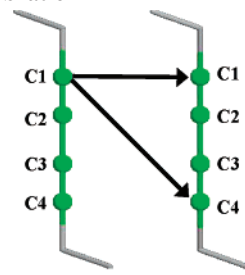
As in previous SAMs studies by Harrison and co-workers,[22,24,27,28] the potential energy function used in this work was the adaptive intermolecular reactive empirical bond-order potential (AIREBO).[21] This potential was parametrized to model hydrocarbon systems of all phases, includes long-range interactions, and retains the unique ability of its antecedent, the REBO potential,[35,36] to model chemical reactions. Thus, chemical reactions that may accompany compression and sliding are possible in this model.

The end-chain and perpendicular-chain monolayers are composed of $-C_{14}H_{28}-C{\equiv}C-C{\equiv}C-C_2H_5$ and $-C_8H_{16}-C{\equiv}C-C{\equiv}C-C_8H_{17}$ chains, respectively. The tilted-chain system is composed of $-C_7H_{14}-C{\equiv}C-C{\equiv}C-C_8H_{17}$ chains. All systems were equilibrated to 300 K. After equilibration, an equilibrated amorphous tip was added approximately 5 Å above each monolayer, where the potential between the probe and the monolayers is essentially zero. Load was applied to the monolayers by moving the probe at a constant velocity of 0.2 Å/ps toward the monolayers. Prior to sliding, configuration files were extracted at the desired loads and a second equilibration was performed. Sliding was accomplished by moving the rigid layer of the tip at constant velocity (0.2 Å/ps) in the chosen sliding direction. The initial sliding directions were chosen to correspond with the tilt of the diacetylene moieties and are given in Figure 1b,c,e. For each monolayer, additional sliding simulations were also conducted in the directions transverse to the initial sliding directions. The average frictional response at each load was obtained by shearing the films for 10 unit cells, discarding data from the first three unit cells to exclude startup effects, then averaging the friction and load over the remaining unit cells. The unit cell that was used was that of the underlying (2 × 2) diamond (111) substrate.

Results

Compression of Monolayers. Each alkyne chain contains one diacetylene moiety and the remaining carbon atoms are sp^3-

TABLE 1: Average Distances between Carbon Atoms in Chains after Equilibration[a]

	Perpendicular Chains $-C_8H_{16}-C{\equiv}C-C{\equiv}C-C_8H_{17}$	Tilted-Chains $-C_7H_{14}-C{\equiv}C-C{\equiv}C-C_8H_{17}$
C1 – C1	5.0 Å (4.7 Å)	5.00 Å (4.8 Å)
C1 – C4	5.0 Å (4.1 Å)	4.7 Å (4.2 Å)

[a] Distances under 200 nN of load are shown in parentheses.

hybridized. The UV-initiated polymerization of diacetylene crystals and films proceeds by the following mechanism.[16,18] Consider a single diacetylene chain, carbon atom one (C_1 in Table 1) reacts with carbon atom four (C_4) on an adjacent chain. At the same time, C_4 on this initial chain reacts with C_1 on a third, adjacent chain. The result is a long chain of conjugated π bonds (sp^2- and sp-hybridized carbon atoms). Thus, the formation of sp^2-hybridized carbon, which is indicative of a double bond being formed between adjacent chains, was used to identify cross-linking (polymerization) in these simulations. The hybridization of a given carbon atom was determined by analyzing the number of neighbors of each atom. The average postequilibration distances between atoms C_1 and C_4 on adjacent chains are given in Table 1 for two of the monolayers examined here. The C_1-C_1 distances are within the range reported by Menzel et al.[8,11] whereas the C_1-C_4 distances are a bit longer than the range of 3.4−4.0 Å given in the literature.

The spacer length alters the relative orientation of the diacetylene and tail portions of the chains relative to the surface normal of the diamond substrate. When viewed along the same direction (Figure 1a,e), the diacetylene and tail regions of the chains appear approximately perpendicular to the diamond substrate in the systems with an even number of carbon atoms in the spacer regions, i.e., perpendicular- and end-chain monolayers. A spacer with an odd number of carbon atoms causes the diacetylene region of the chains to be canted with respect to the surface normal when viewed along both directions, i.e., tilted-chain monolayer (Figure 1c,d).

The tip was moved toward the monolayers at 0.2 Å/ps until the load on the tip was approximately 200 nN. A plot of the number of sp^2-hybridized carbon atoms formed during compression versus load is shown in Figure 2 for all the monolayers examined here. The application of load causes displacement between adjacent chains within the monolayers, and as a result, some chains are "squeezed" together. Consequently, the average C_1-C_1 and C_1-C_4 distances between chains are reduced with the average C_1-C_4 distances (Table 1) becoming very close to range reported in the literature.[8,11]

It is clear from analysis of these data that once the formation of sp^2-hybridized carbon is initiated, it increases with load. Over almost the entire load range examined, the extent of the polymerization is the largest in the end-chain system. In the tilted-chain system, because the spacer length differs from the perpendicular-chain monolayer, the diacetylene moieties are in
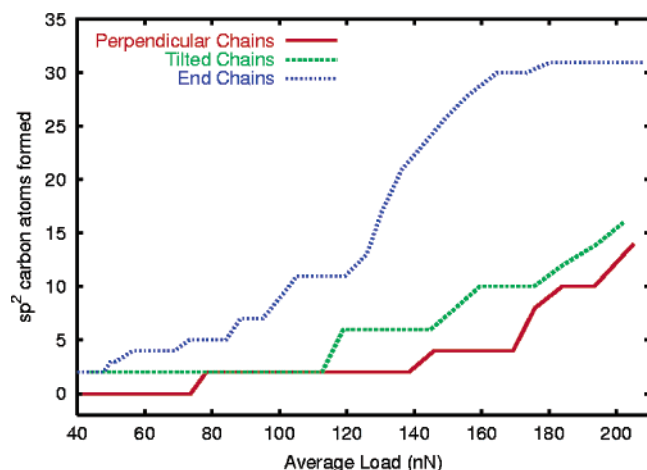
Figure 2. Number of sp^2-hybridized carbon atoms in the monolayers examined here as a function of load.
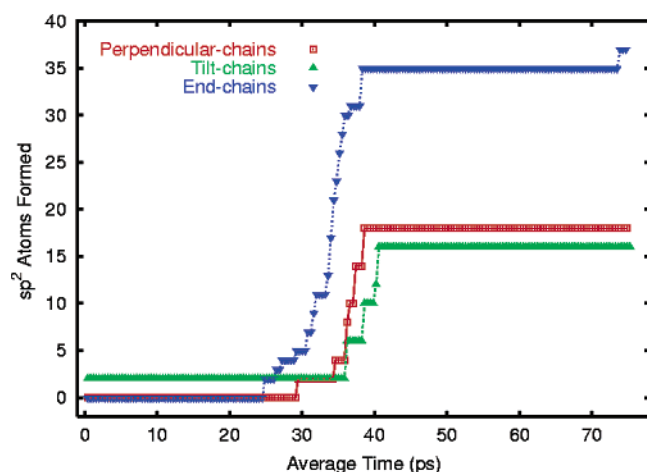

Figure 3. Number of sp^2-hybridized carbon atoms in the monolayers as a function of simulation time. These data correspond to compression and pullback of the tip. Pull-back begins at 37.5, 40.6, and 37.9 ps in the perpendicular-, titled-, and end-chain systems, respectively.

a slightly different orientation. As a result, a few cross-links are formed during the equilibration process. Loads in excess of 110 nN result in increased polymerization. Although the polymerization of the tilted-chain monolayer is slightly larger than the perpendicular-chain monolayer at loads in excess of 110 nN, the difference between these two systems is quite small at the maximum compression studied (200 nN).

The number of sp^2-hybridized carbon atoms was plotted as a function of time for compression and pull-back of the tip (Figure 3). The pull-back begins at the point of maximum compression and stops when the interaction potential between the tip and the monolayer has effectively gone to zero. These data show that polymerization is preserved upon pull-back of the tip from the monolayers; i.e., it is irreversible. Snapshots of each monolayer after compression and pull-back show the sustained polymerization in all films (Figure 4). It is clear from analysis of these snapshots that there are more reactions between chains in the end-chain monolayer. In addition, due to the proximity of the triple-bond region to the ends of the chains, reactions also occur between the monolayer and the amorphous carbon tip. The formation of these tip−monolayer bonds results in chains being pulled from the substrate as the tip was pulled back. This leads to damage of the monolayer and to some material transfer to the tip. In contrast, no reactions occur between the tip and the perpendicular- or the tilted-chain monolayers.

Sliding Induced Changes. System configurations for each monolayer were extracted from the compression simulations and equilibrated until the potential energy of the system reached a steady-state value. The tip was then moved along the chosen sliding direction for 10 unit cells and the frictional response of the monolayers determined. Figure 5 shows the average friction, and the number of sp^2-hybridized carbon atoms formed, as a function of sliding distance in the perpendicular-, tilted- and the end-chain monolayers under a load of approximately 150 nN.

When sliding is in the x direction, the average friction of the perpendicular-chain system increases slightly, experiences a marked drop (dip), and then increases again during the first 10 Å of sliding (Figure 5a). This "dip" in the friction is present when sliding the perpendicular-chain system at all loads. After the initial fluctuations, the friction oscillates about some average value for the remainder of the slide. In contrast, the number of sp^2-hybridized carbon atoms formed increases steadily with sliding distance. Thus, there is no correlation between the number of sp^2-hybridized carbon atoms formed and the average friction during sliding in this system. In fact, sliding initiates further polymerization in all of the monolayers examined here; however, none of them show a concomitant increase in friction (Figure 5b,c).

The "dip" in the friction (Figure 5a) arises from the collective reorientation of the spacer region of the chains within the perpendicular-chain monolayer during sliding. The initial sliding directions were chosen to correspond to the tilt direction of the diacetylene moieties within the chains. It is clear from an analysis of Figure 1b that sliding from right-to-left corresponds to the direction of the diacetylene tilt ($-x$ direction). In contrast, the spacer region of the chains is not tilted in the sliding direction. This is also apparent from examination of the orientation of the spacer region of the chains looking "down" through the monolayer onto the substrate (Figure 6a). Prior to sliding, the spacer region of the chains is oriented at 90° to the sliding direction. The dip in the friction is caused by the collective reorientation of the spacer region of the chains (Figure 6b) during the initial stages of sliding. This hypothesis was checked by sliding the tip in the direction of the tilt of the spacer region (y direction). In this case, no "dip" in the average friction is observed (Figure 5a) and the spacer region of the chains does not change orientation. After this collective reorganization of the spacer region of the chains when sliding is in the $-x$ direction, the average friction is fairly constant for the remainder of the sliding simulation (Figure 5a).

In the tilted-chain monolayer, once sliding begins in the initial sliding direction (y direction), the average value of the friction increases steadily until it reaches a steady-state value (Figure 5b). Examination of the spacer region of the chains in this monolayer reveals that this portion of the chains is aligned in the sliding direction (Figure 6c). Thus, sliding does not initiate a reorientation of this portion of the chains (Figure 6d). As a result, there is no "dip" in the average friction during the initial stages of sliding. In this system, sliding transverse to the initial sliding direction (x direction) does not cause a collective reorientation of the spacer region of the chains. Thus, there is no marked "dip" in the average friction data (Figure 5b). However, the spacer portions of some chains within the monolayer do reorient (Figure 6e). Close examination of the conformation after sliding reveals that orientation of the spacer region of the chains is not uniform (Figure 6e) as it is in the perpendicular-chain system when sliding is in the $-x$ direction (Figure 6b). The average friction when sliding is in the x
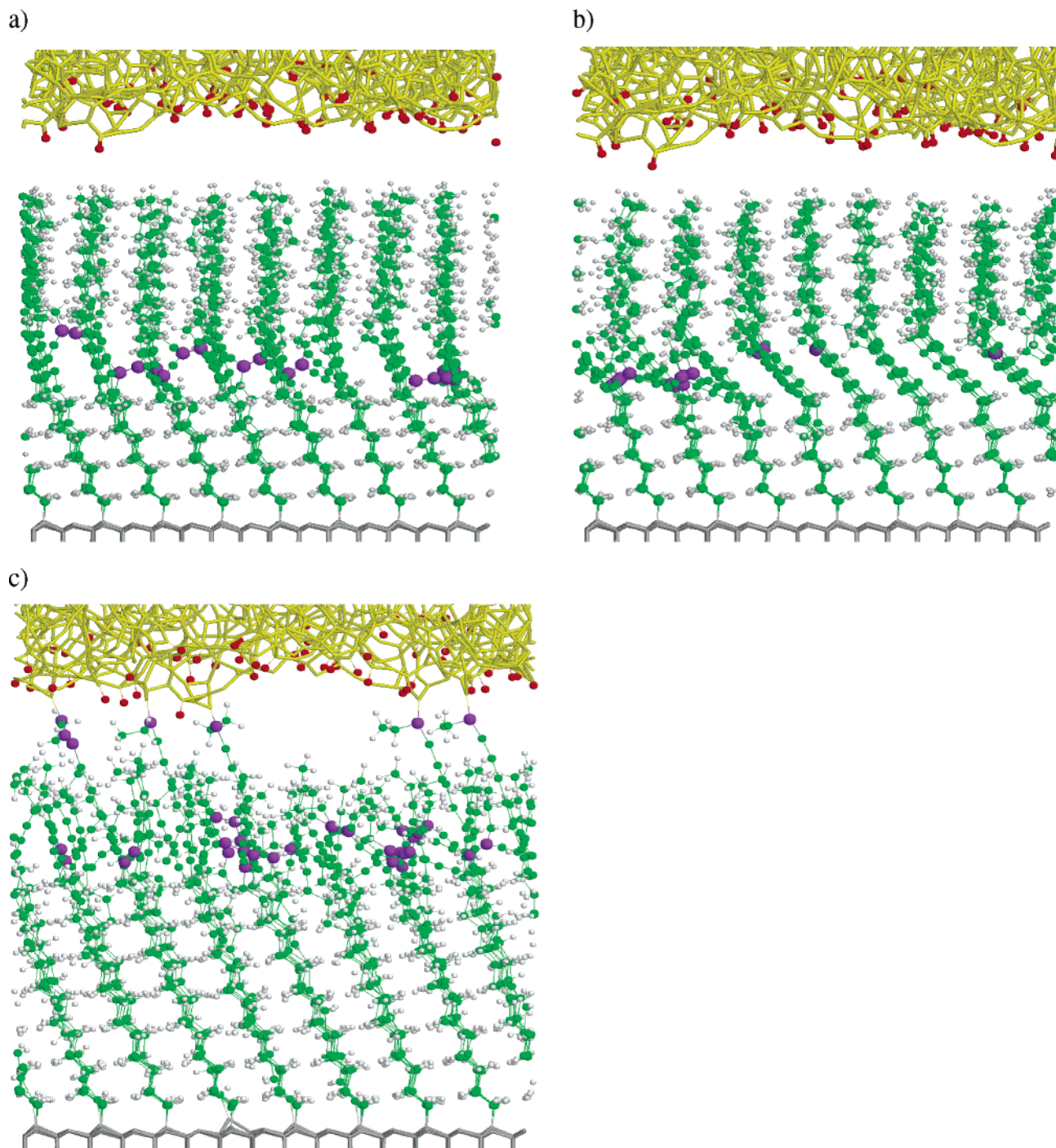
a)

b)

c)

Figure 4. Perpendicular- (a), tilted- (b), and end-chain (c) monolayer systems after compresssion to 200 nN and tip pull-back. Color coding is as in Figure 1 except that cross-linked atoms (sp^2-hybridized) are shown as purple spheres.

direction is somewhat higher (Figure 5b) than it is in the *y* direction. The partial reorientation of the spacer potion of some of the chains takes place during the first 25 Å of sliding. After the partial reorientation, the average friction for sliding in this direction is very close to that for sliding in the *y* direction.

It is also worth noting that approximately the same number of sp^2-hybridized carbon atoms is formed during sliding in the tilted-chain system compared to the perpendicular-chain system at this load. However, this is not the case at approximately 200 nN where 65 and 40 sp^2-hybridized carbon atoms are formed in the tilted-chain and the perpendicular-chain monolayers, respectively.

In the end-chain system, the friction rises sharply for the first 20 Å of sliding. Compression of this monolayer, and sliding, result in the formation of adhesive interactions, or covalent bonds, between the tip and the monolayer. The existence of these adhesive bonds causes a buildup of stress during the first 20 Å of sliding. During this time, additional adhesive bonds are formed but none are severed. After 20 Å of sliding, the stress is such that these adhesive bonds begin breaking. Severing these bonds causes significant changes in the chemical makeup of the tip and the monolayer. Bonds are broken and formed for the remainder of the slide as the nature of the tip and the monolayer are changed (Figure 7c). Friction decreases as sliding
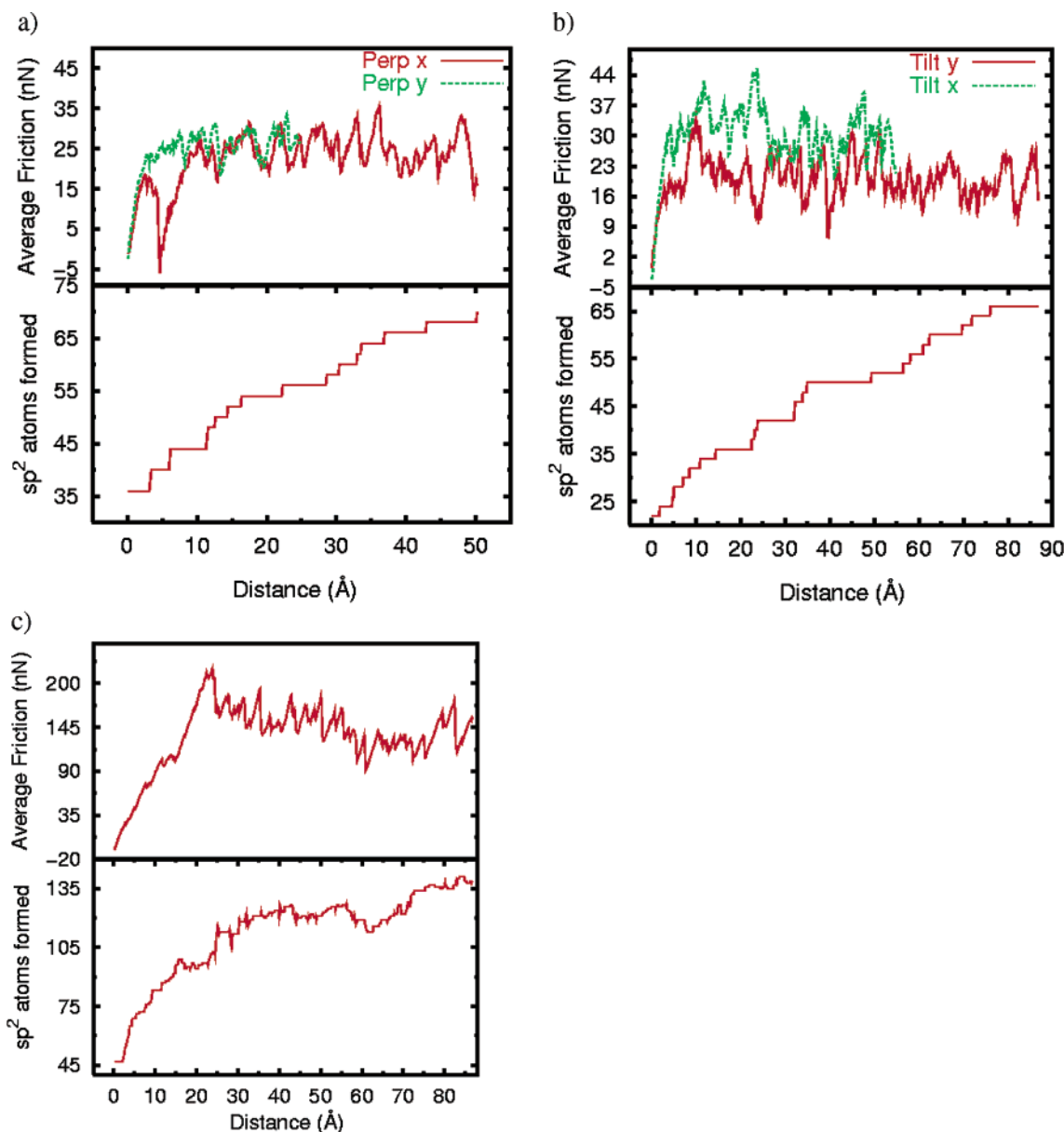
Polymerization in Diacetylene-Containing Monolayers

J. Phys. Chem. B, Vol. 108, No. 43, 2004 **16631**

Figure 5. Average friction and number of sp^2-hybridized carbon atoms in the (a) perpendicular-, (b) tilted-, and (c) end-chain monolayers as a function of sliding distance. The load is approximately 150 nN in all the systems. Sliding directions are given in the text.

progresses during the remainder of the simulation. A correlation between the breaking and making of bonds and friction has also been observed in our previous simulations.[37,38]

The changes in the numbers of sp^2-hybridized carbons for the end-chain system during sliding are much larger than for the perpendicular system (Figure 5c). There are more reactions between chains in the end-chain system. In addition, there are chemical reactions between the tip and the monolayer. No reactions occur between the tip and the monolayer in the perpendicular- or the tilted-chain systems. Due to the proximity of the diacetylene moieties to the tip in the end-chain system, the tip reacts with the monolayer. Analysis of the changes in the hybridization of the carbon atoms of the tip while it is in sliding contact with the end-chain monolayer reveals that the number of sp-hybridized carbon atoms in the tip is significantly reduced during the sliding whereas the number of sp^3- and sp^2-hybridized atoms remains fairly constant. When the tip is in sliding contact with the perpendicular-chain monolayer, the number of sp-hybridized carbon atoms in the tip decreases whereas the number of sp^2-hybridized carbon atoms increases. Thus, the net effect on the tip when in sliding contact with the

perpendicular-chain system is the conversion of sp- into sp^2-hybridized carbon.

Though the orientation of the spacer region impacts the average friction, the nature of the sliding interface also has a profound influence on the friction. Figure 7 shows the monolayer systems examined here after 10 unit cells (the unit cell is that of the diamond substrate) of sliding. In the perpendicular- and tilted-chain systems, the region of the chains in contact with the tip (tail region) is quite disordered whereas the spacer region remains somewhat ordered. In the end-chain system, chemical bonds between the tip and the monolayer are apparent.

Both the application of load and of shear induce polymerization, or cross-linking, of the chains. The cross-linking patterns for the perpendicular- and tilted-chain systems are shown in Figure 8, after the tip has been slid 10 unit cells. Both systems are under the highest loads examined here (200 nN). In the perpendicular-chain system, the application of shear produces an irregular pattern of cross-linking between chains. Although there are a large number of cross-links formed between C_1-C_4 (40.0%), there are also significant numbers of bonds formed between C_1-C_2 (12.7%), C_2-C_4 (14.5%), and C_3-C_4 (14.5%).
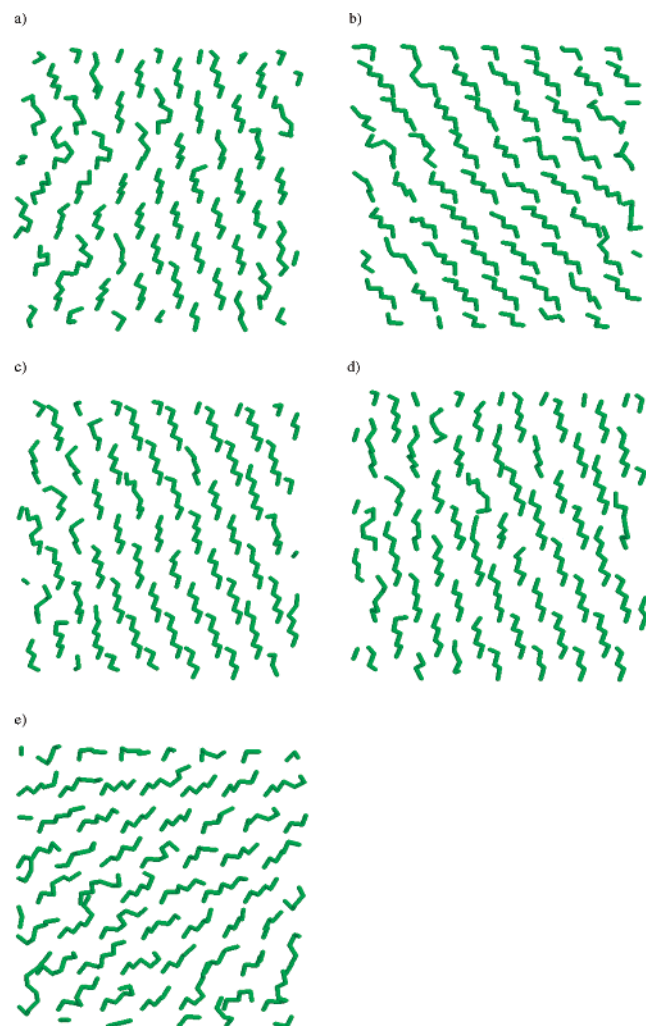
a)

b)

c)

d)

e)

Figure 6. Spacer region of the perpendicular-chain system under 200 nN of load before sliding in (a) and after sliding (b) for 20 ps in the −x direction. Spacer region of the tilted-chain system under 200 nN of load prior to sliding in (c), after sliding 45 ps in the y direction (d), and after sliding 45 ps in the x direction (e). Sliding direction is from right-to-left in (a) and (b), bottom-to-top in (c) and (d), and from left-to-right in (e). All atoms but the carbon atoms (green) of the spacer regions of the chains have been omitted for clarity.
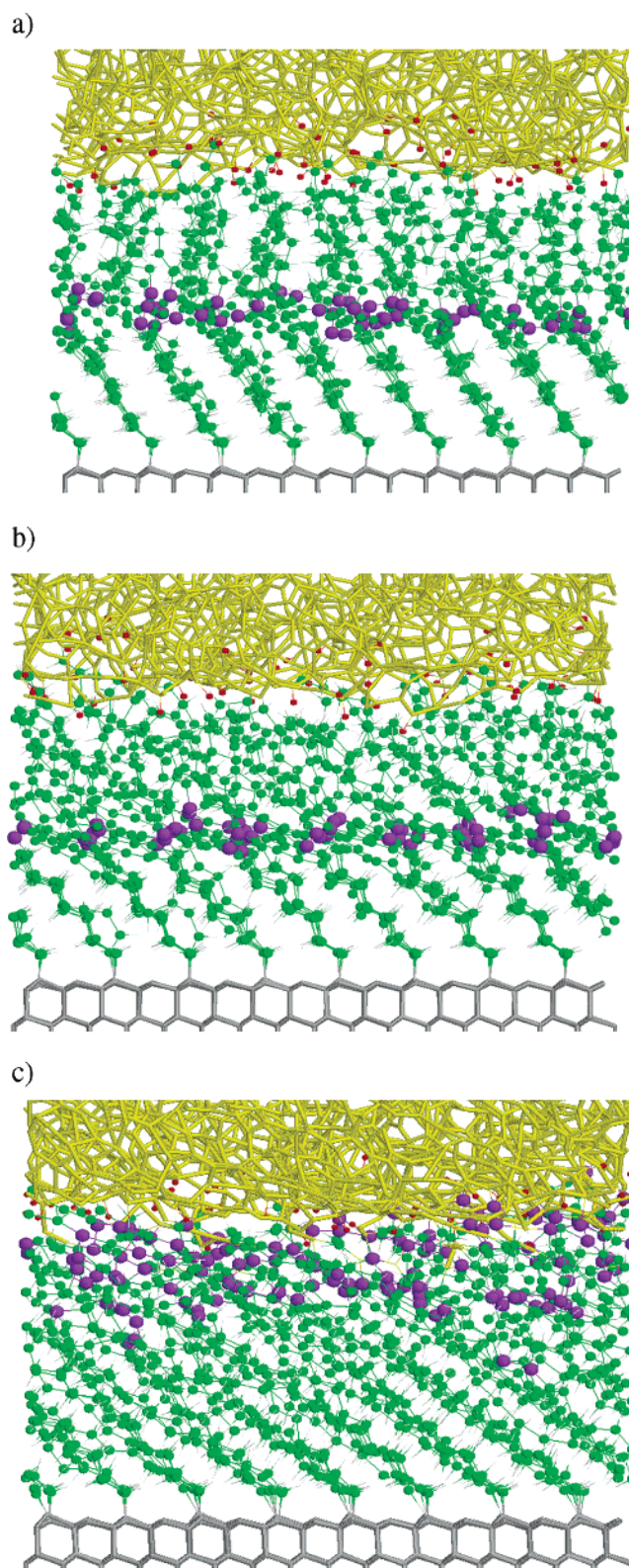
a)

b)

c)

Figure 7. Perpendicular- (a), tilted- (b), and end-chain (c) monolayer systems after 10 unit cells of sliding under a load of approximately 150 nN. The sliding direction is from back-to-front (−x) in (a) and from right-to-left (y) in (b) and (c). The colors are the same as in Figure 4.

In addition, the tail and polymerized regions are at an angle of approximately 45° to the sliding direction (Figure 6b). This is a byproduct of the even spacer length and the sliding direction (x direction).

In the tilted-chain system, the polymerization pattern is different than that obtained in the perpendicular-chain system. That is, the majority of the bonds are formed between C_1-C_4 (53.2%). The other major contributors to the polymerization in this system are C_1-C_1 (14.9%) and C_1-C_2 (17.0%). In addition, there is a small degree of conjugation of the π bonds and the chains are generally aligned with (parallel to) the sliding direction. This alignment is a result of the odd spacer length and the sliding direction. In this case, the spacer is aligned in the sliding direction (Figure 6c). Thus, the entire chain can align itself with the sliding direction. This pattern of cross-linking has some similarity to the proposed cross-linking initiated by UV excitation of diacetylene films because the majority of the cross-links are between C_1 and C_4. However, the carbon backbones produced by UV excitation are much longer than those produced by shearing. In addition, UV excitation produces cross-links only between atoms C_1 and C_4 whereas all the carbon

atoms within the diacetylene moieties can form cross-links during shear-induced polymerization.

In the end-chain system, a number of cross-linking patterns are observed. In contrast to the cross-linking observed in the other two systems examined here and after UV excitation of
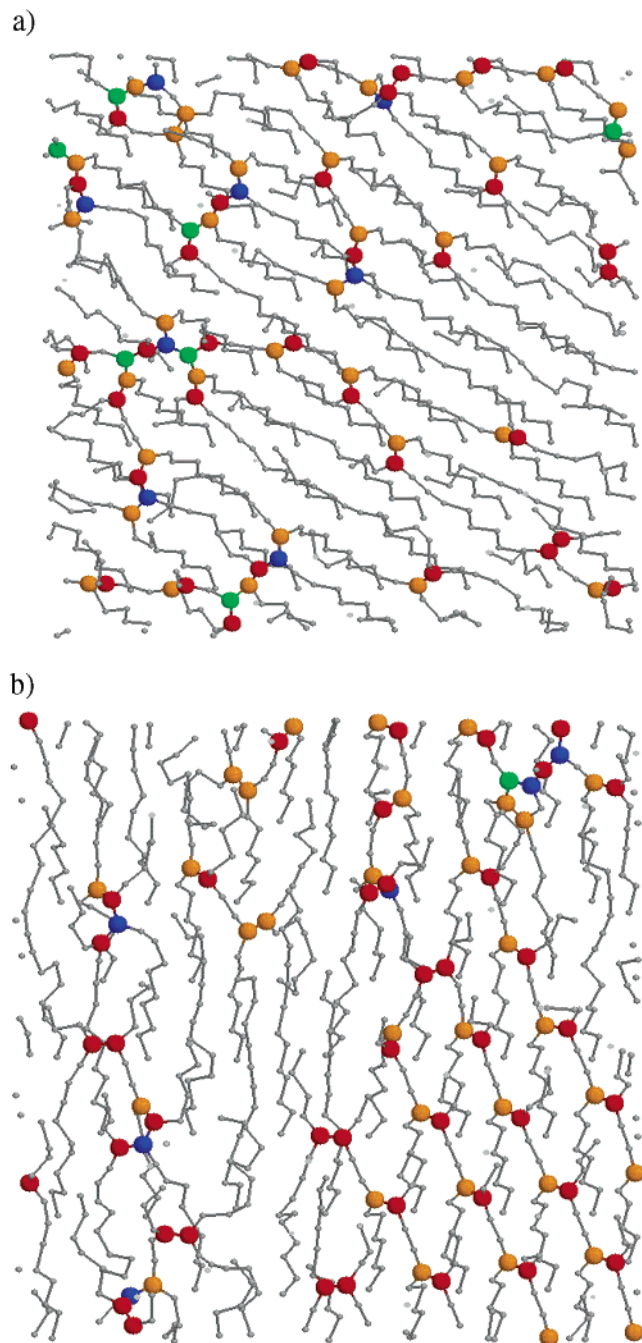
a)

b)

Figure 8. Top-view of the (a) perpendicular- and (b) tilted-chain monolayers after 10 unit-cells of sliding under approximately 200 nN of load. Alkyne chains are shown as gray sticks and spheres. Carbon atoms 1−4 of the diacetylene moieties are colored red, blue, green, and orange, respectively. The diamond substrate and tip are not shown for clarity. The sliding direction is from right-to-left ($-x$) and from bottom-to-top (y) in the upper and lower panels, respectively.
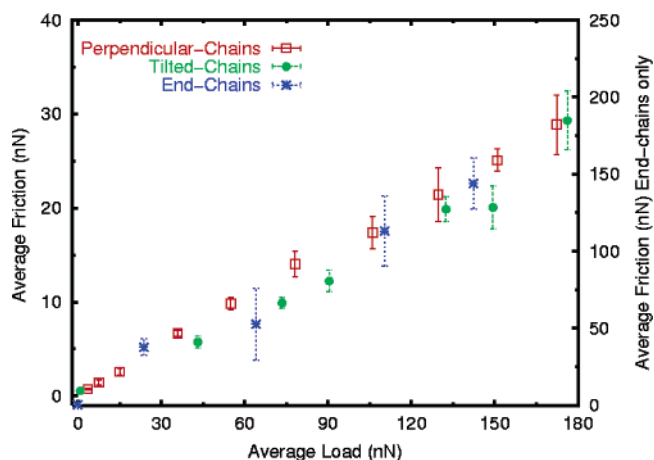

Figure 9. Average friction as a function of average load for the monolayer systems examined here. Scale for the average friction in the end-chain system is shown on the right-hand-side of the figure. Sliding directions are the $-x$ for the perpendicular-chain system and y for the other two monolayers.

diacetylene films, it is possible to induce cross-links between multiple chains. As a result, rings of atoms on the ends of the chains can be formed.

The dependence of the cross-linking pattern on sliding direction was examined in the perpendicular- and the tilted-chain monolayers. Sliding transverse to the initial sliding direction (x direction or from left-to-right in Figure 1d) in the tilted-chain monolayer changes the cross-linking pattern. The majority of the bonds formed are still between C_1-C_4; however, the percentage of these bonds decreases to 32.8%. The other major contributors to the polymerization for this sliding direction are C_1-C_1 (12.5%), C_1-C_2 (14.1%), and C_1-C_3 (15.6%). In

addition, the C_1-C_4 are no longer aligned in the sliding direction. Thus, the relative orientations of the spacer region and the diacetylene moieties relative to the surface normal, in conjunction with the sliding direction, have a marked influence on the pattern of shear-induced polymerization.

Friction. Load versus friction data for the end-, tilted-, and perpendicular-chain systems are shown in Figure 9. The frictional response for the end-chain system is roughly 10 times larger than that of the other two monolayer systems. This arises from the adhesive interactions (covalent bonds) between the film and tip. There are no adhesive interactions between the tip and the monolayer in the perpendicular- or tilted-chain systems. Thus, the friction measured in these systems is a wearless friction. The average friction versus load is the same for the tilted- and perpendicular-chain systems. These two monolayers have the same packing and number of carbon atoms in the tail regions. Thus, the interactions with the tip are similar and so is the average friction. It should also be noted that in the absence of start-up effects (Figure 5a,b), there is no friction anisotropy in the perpendicular- or tilted-chain systems.

Conclusions

Molecular dynamics and the AIREBO potential have been used to examine the compression and shear of diacetylene-containing chains covalently bound to diamond. These simulations show that cross-linking, or polymerization, between chains is initiated by the mechanical deformation of the monolayers. Both the application of load and shear led to polymerization between chains. To our knowledge, these simulations are the first reported observation of this behavior.

In this work, three monolayer systems were examined that differed in the location of the diacetylene moieties within the chains. The unsaturated region was placed at the ends of the chains, closest to the tip, in the end-chain monolayers and in the middle of the chains in the perpendicular- and tilted-chain monolayers. The spacer length differed by one carbon atom in the perpendicular- (C_8) and tilted-chain (C_7) monolayers, and the tail lengths (C_8) were equal. When this diacetylene-containing region is on the ends of the chains, significant, irregular cross-linking occurs between chains and between the tip and the chains. In contrast, when the sp-hybridized region is far from the interface, no chemical bonds form between the tip and the chains. The formation of covalent bonds between

the tip and the monolayer causes the frictional response of the end-chain monolayer to be significantly larger than for the other two monolayers.

Altering the spacer length by one carbon atom causes the orientation of the diacetylene-containing region and the tail region of the chains to differ relative to the sliding direction. The chains in the tilted-chain system ($-C_7-$) possess only one cant in the initial sliding direction (*y* direction). That is, the all trans configuration of the spacer region of the chains and the diacetylene moieties have the same cant. The tail regions of the chains are nearly perpendicular to the surface normal (Figure 1c). When viewed in the transverse direction (Figure 1d), the cant of the chains is very close to the surface normal. In the perpendicular-chain monolayer (Figure 1a), the even number of carbon atoms ($-C_8-$) in the spacer region of the chains causes a "kink" in the chains. That is, the cant of the spacer region is not in the same direction as the cant of the diacetylene moieties (Figure 1b). This change in orientation results in minor differences in the number of cross-links upon the application of load, and shear, with the most significant differences found in the patterns of polymerization and the friction response at startup.

The length of the spacer region and the sliding direction influence the three-dimensional cross-linking pattern between chains formed during shear. When sliding in the *x* direction, the "kink" in the chains of the perpendicular-chain monolayer causes the number of C_1-C_4 bonds formed to be much less than in the tilted-chain system. The kink also prevents the alignment of the chains in the sliding direction. The resulting structure possessed a fragmented carbon backbone. It should be noted that the shear-induced polymerization in both the tilt- and perpendicular-chain systems is quite different from the polymerization induced when diacetylene films are exposed to UV radiation. Experimental studies have confirmed that UV excitation of diacetylene crystals and monolayers produces long π-conjugated carbon backbones with bonds forming between C_1 and C_4 on adjacent chains making long, regular rows of polymerized chains.[9−11,15,16,18,39]

The friction versus load response for each monolayer was linear. In the perpendicular- and tilted-chain systems, the friction was approximately 10 times greater than what was reported in previous MD studies of a flat tip (hydrogen-terminated diamond) sliding over monolayers composed of alkane chains,[22] and approximately 100 times less than in the end-chain system. The large frictional response in the end-chain system was due to chemical reactions between the tip and the monolayer, induced by compression and shear. In the tilted- and perpendicular-chain systems, the diacetylene-containing region within the chains is far from the interface, and the tails of each chain all contain 8 carbon atoms. Because there are no chemical reactions between the tip and the chains, the friction is a wearless friction. In addition, these simulations show that cross-linking that occurs during sliding far from the tip−monolayer interface does not influence the average friction. Thus, it is likely that the origin of the difference in the friction between the tilted- and perpendicular-chain systems examined here, compared to the alkane-containing monolayers[22] examined previously, is largely due to the amorphous carbon tip used here. (Preliminary simulations confirm this conclusion.) This tip is incommensurate with the monolayers, and its surface is rough on the atomic scale. Thus, it introduces significant disorder in the tail region of the diacetylene-containing chains during compression and sliding. In contrast, compression of alkane-containing chains of a single length yields a very ordered system in which all

chains have a similar response during sliding.[22,24] Both simulations[22,40] and experiments[41] have shown that disordered systems have higher friction than ordered systems.

References and Notes

(1) Tachibana, H.; Yamanaka, Y.; Sakai, H.; Abe, M.; Matsumoto, M. Effect of Position of Butadiyne Moiety in Amphiphilic Diacetylenes on Polymerization in the Langmuir−Blodgett Films. *Macromolecules* **1999**, *32*, 8306−8309.

(2) Carpick, R. W.; Mayer, T. M.; Sasaki, D. Y.; Burns, A. R. Spectroscopic Ellipsometry and Fluorescence Study of Thermochromism in an Ultrathin Poly(diacetylene) Film: Reversibility and Transition Kinetics. *Langmuir* **2000**, *16*, 4639−4647.

(3) Sasaki, D. Y.; Carpick, R. W.; Burns, A. R. High Molecular Orientation in Mono- and Trilayer Polydiacetylene Films Imaged by Atomic Force Microscopy. *J. Colloid Interface Sci.* **2000**, *229*, 490−496.

(4) Lio, A.; Reichert, A.; Ahn, D. J.; Nagy, J. O.; Salmeron, M.; Charych, D. H. Molecular Imaging of Thermochromic Carbohydrate-Modified Polydiacetylene Thin Films. *Langmuir* **1997**, *13*, 6524−6532.

(5) Carpick, R. W.; Sasaki, D. Y.; Burns, A. R. First Observation of Mechanochromism at the Nanometer Scale. *Langmuir* **2000**, *16*, 1270−1278.

(6) Evans, S. D.; Goppert-Berarducci, K. E.; Urankar, E.; Gerenser, L. J.; Ulman, A. Monolayers Having Large In−Plane Dipole Moments: Characterization of Sulfone-Containing Self-Assembled Monolayers of Alkanethiols on Gold by Fourier Transform Infrared Spectroscopy, X-ray Photoelectron Spectroscopy, and Wetting. *Langmuir* **1991**, *7*, 2700−2709.

(7) Mowery, M. D.; Menzel, H.; Cai, M.; Evans, C. E. Fabrication of Monolayers Containing Internal Molecular Scaffolding: Effect of Substrate Preparation. *Langmuir* **1998**, *14*, 5594−5602.

(8) Menzel, H.; Mowery, M. D.; Cai, M.; Evans, C. E. Vertical Positioning of Internal Molecular Scaffolding within a Single Molecular Layer. *J. Phys. Chem. B* **1998**, *102*, 9550−9556.

(9) Menzel, H.; Mowery, M. D.; Cai, M.; Evans, C. E. Fabrication of Noncovalent and Covalent Internal Scaffolding in Monolayer Assemblies Using Diacetylenes. *Macromolecules* **1999**, *32*, 4343−4350.

(10) Cai, M.; Mowery, M. D.; Menzel, H.; Evans, C. E. Fabrication of Extended Conjugated Length Polymers within Diacetylene Monolayers on Au Surfaces: Influence of UV Exposure Time. *Langmuir* **1999**, *15*, 1215−1222.

(11) Menzel, H.; Horstmann, S.; Mowery, M. D.; Cai, M.; Evans, C. E. Diacetylene Polymerization in Self-Assembled Monolayers: Influence of the Odd/Even nature of the Methylene Spacer. *Polymer* **2000**, *41*, 8113−8119.

(12) Mowery, M. D.; Smith, A. M.; Evans, C. E. Polydiacetylene Monolayers as Versatile Photoresists for Interfacial Patterning. *Langmuir* **2000**, *16*, 5998−6003.

(13) Burns, A. R.; Carpick, R. W.; Sasaki, D. Y.; Shelnutt, J. A.; Haddad, R. Shear-induced Mechanochromism in Polydiacetylene Monolayers. *Tribol. Lett.* **2001**, *10* (1−2), 89−96.

(14) Cheadle, E. M.; Batchelder, D. N.; Evans, S. D.; Zhang, H. L.; Fukushima, H.; Miyashita, S.; Graupe, M.; Puck, A.; Shmakova, O. E.; Colorado, R., Jr.; Lee, T. R. Polymerization of Semi-Fluorinated Alkane Thiol Self-Assembled Monolayers Containing Diacetylene Units. *Langmuir* **2001**, *17*, 6616−6621.

(15) Evans, C. E.; Smith, A. C.; Burnett, D. J.; Marsh, A. L.; Fischer, D. A.; Gland, J. L. Polymer Conversion Measurement of Diacetylene-Containing Thin Films and Monolayers Using Soft X-ray Fluorescence Spectroscopy. *J. Phys. Chem. B* **2002**, *106*, 9036−9043.

(16) Enkelmann, V. Structural Aspects of the Topochemical Polymerization of Diacetylenes. *Adv. Polym. Sci.* **1984**, *63*, 91−136.

(17) Nallicheri, R. A.; Rubner, M. F. Influence of Cross-Linking on the Hysteresis Behavior of Poly(urethane-diacetylene) Segmented Copolymers. *Macromolecules* **1991**, *24*, 526−529.

(18) Bloor, D.; Chance, R. R. *Polydiacetylenes: Synthesis, Structure, adn Electronic Properties*; Nijhoff: Dordrecht, 1985.

(19) Mowery, M. D.; Kopta, S.; Ogletree, D. F.; Salmeron, M.; Evans, C. E. Structural Manipulation of the Frictional Properties of Linear Polymers in Single Molecular Layers. *Langmuir* **1999**, *15*, 5118−5122.

(20) Carpick, R. W.; Sasaki, D. Y.; Burns, A. R. Large Friction Anisotropy of a Polydiacetylene Monolayer. *Tribol. Lett.* **1999**, *7*, 79−85.

Polymerization in Diacetylene-Containing Monolayers

J. Phys. Chem. B, Vol. 108, No. 43, 2004 **16635**

(21) Stuart, S. J.; Tutein, A. B.; Harrison, J. A. A Reactive Potential for Hydrocarbons with Intermolecular Interactions. *J. Chem. Phys.* **2000**, *112*, 6472−6486.

(22) Mikulski, P. T.; Harrison, J. A. Packing-Density Effects on the Friction of *n*-Alkane Monolayers. *J. Am. Chem. Soc.* **2001**, *123*, 6873−6881.

(23) Fenter, P.; Eberhardt, A.; Eisenberger, P. Self-Assembly of *n*-Alkyl Thiols as Disulfides on Au(111). *Science* **1994**, *266*, 1216.

(24) Mikulski, P. T.; Harrison, J. A. Periodicities in the Properties Associated with the Friction of Model Self-Assembled Monolayers. *Tribol. Lett.* **2001**, *10*, 29−38.

(25) Harrison, J. A.; White, C. T.; Colton, R. J.; Brenner, D. W. Investigation of the Atomic-scale Friction and Energy Dissipation in Diamond using Molecular Dynamics. *Thin Solid Films* **1995**, *260*, 205−211.

(26) Perry, M. D.; Harrison, J. A. Universal Aspects of the Atomic-Scale Friction of Diamond Surfaces. *J. Phys. Chem.* **1995**, *99*, 9960−9965.

(27) Tutein, A. B.; Stuart, S. J.; Harrison, J. A. Indentation Analysis of Linear-Chain Hydrocarbon Monolayers Anchored to Diamond. *J. Phys. Chem. B* **1999**, *103*, 11357−11365.

(28) Tutein, A. B.; Stuart, S. J.; Harrison, J. A. Role of Defects in the Compression and Friction of Anchored Hydrocarbon Chains on Diamond. *Langmuir* **2000**, *16*, 291−296.

(29) Berendsen, H. J. C.; Postma, J. P. M.; van Gunsteren, W. F.; DiNola, A.; Haak, J. R. Molecular dynamics with coupling to an external bath. *J. Chem. Phys.* **1984**, *81*, 3684−3690.

(30) van der Ploeg, P.; Berendsen, H. J. C. Molecular dynamics simulation of a bilayer membrane. *J. Chem. Phys.* **1982**, *76*, 3271−3276.

(31) Verlet, L. *Phys. Rev. B* **1967**, *159*, 98.

(32) Gao, G.-T.; Mikulski, P. T.; Chateauneuf, G. M.; Harrison, J. A. The Effects of Film Structure and Surface Hydrogen on the Properties of Amorphous Carbon Films. *J. Phys. Chem. B* **2003**, *107*, 11082−11090.

(33) Gao, G. T.; Mikulski, P. T.; Harrison, J. A. Molecular-Scale Tribology of Amorphous Carbon Coatings: Effects of Film Thickness, Adhesion, and Long-Range Interactions. *J. Am. Chem. Soc*. **2002**, *124*, 7202−7209.

(34) Glosli, J.; Ree, F. H. Liquid−liquid-phase transformtion in carbon. *Phys. Rev. Lett.* **1999**, *82*, 4659−4662.

(35) Brenner, D. W.; Shenderova, O. A.; Harrison, J. A.; Stuart, S. J.; Ni, B.; Sinnott, S. B. Second Generation Reactive Empirical Bond Order (REBO) Potential Energy Expression for Hydrocarbons. *J. Phys. C.* **2002**, *14*, 783−802.

(36) Brenner, D. W. Empirical potential for hydrocarbons for use in simulating the chemical vapor deposition of diamond films. *Phys. Rev. B* **1990**, *42*, 9458−9471.

(37) Gao, G. T.; Mikulski, P. T.; Harrison, J. A. Molecular-Scale Tribology of Amorphous Carbon Coatings: Effects of Film Thickness, Adhesion, and Long-Range Interactions. *J. Am. Chem. Soc.* **2002**, *124*, 7202−7209.

(38) Gao, G. T.; Mikulski, P. T.; Chateauneuf, G. M.; Harrison, J. A. The Effects of Film Structure and Surface Hydrogen on the Properties of Amorphous Carbon Films. *J. Phys. Chem. B* **2003**, *107*, 11082−11090.

(39) Beckham, H. W.; Rubner, M. F. On the Origin of Thermochromism in Cross-Polymerized Diacetylene-Functionalized Polyamides. *Macromolecules* **1993**, *26*, 5198−5201.

(40) Mikulski, P. T.; Gao, G.-T.; Chateauneuf, G. M.; Harrison, J. A. Contact Forces at the Sliding Interface: Mixed vs Pure Model Alkane Monolayers. *J. Chem. Phys.*, submittedfor publication.

(41) Lee, S.; Shon, Y.-S.; Colorado, R.; Guenard, R. L.; Lee, T. R.; Perry, S. S. The Influence of Packing Densities and Surface Order on the Frictional Properties of Alkanethiol Self-Assembled Monolayers (SAMs). *Langmuir* **2000**, *16*, 2220−2224.